DEFORMATION AND FRACTURE OF A TITANIUM ALLOY UNDER BI-AXIAL FATIGUE

M.R. BACHE and W.J. EVANS
I.R.C. in Materials for High Performance Applications,
University of Wales, Swansea, West Glamorgan, SA2 8PP, U.K.

ABSTRACT

The effects of bi-axial loading on the fatigue response of the near alpha titanium alloy IMI834 under tension, torsion and combined mixed mode loading are explored. Data from a comprehensive test matrix at ambient temperature under both load/torque control and strain control are presented. The experimental work encompassed a range of waveforms at frequencies from 1 to 10 Hz and explored the effects of hold times at peak stress. On the basis of the von Mises effective stress criterion, there is a marked dependence of fatigue response on stress biaxiality with the uniaxial state promoting shorter cyclic lives compared with pure torsion. Good correlation between the tension and torsion strain control data is demonstrated, however, when a critical plane parameter is used. The implications of this observation, particularly with regard to quasi-cleavage facets that were formed on all the fracture surfaces, is discussed.

KEYWORDS

Tension, torsion, bi-axial, facets, strain accumulation, stress relaxation

INTRODUCTION

The titanium alloy IMI834 (Ti-5.8Al-4Sn-3.5Zr-0.7Nb-0.5Mo-0.35Si-0.06C) is a near alpha system designed specifically for use in the HP compressor of aero gas turbine engines. Under service conditions, the blades and particularly the discs for which it is used experience complex multiaxial states of stress. In contrast, the database on which the design and lifing calculations for such components is based is built largely on uniaxial data. The present paper addresses this limitation by reporting ongoing research into the bi-axial fatigue response of the near alpha alloys in general and IMI834 in particular. Such work is important for titanium alloys because of their anisotropic deformation characteristics and the fact that fatigue crack initiation and the early stages of crack growth are strongly influenced by the orientation of basal planes with respect to the loading axis (Bache and Evans, 1992; Bache et al, 1995a).

The development of subsurface, quasi-cleavage facets under fatigue loading is characteristic of titanium alloys. These facets are frequently found to have a basal plane orientation and under some loading conditions can lie approximately perpendicular to the maximum principal stress axis (Bache et al, 1995a). Previous workers have identified an increased tendency for facet

formation when the fatigue cycle includes a dwell period at peak stress. A number of factors have been invoked to explain their formation including the time dependent accumulation of strain and stress tri-axiality.

The alloy IMI834 was developed to meet the demand for enhanced compressor operating temperatures approaching 650°C. At the same time, it was recognised that improved temperature capability could not be gained at the expense of low temperature fatigue performance. The resultant optimised microstructure has a fine grained, bi-modal morphology consisting of equiaxed primary alpha grains in a fully transformed beta matrix. It was anticipated that this microstructure would also reduce the susceptibility to dwell observed in previous coarse grained near alpha alloys. It was within this scenario that the present programme of research was conceived. The objectives were to explore the ambient temperature fatigue performance, to characterise cyclic deformation and crack development mechanisms and to investigate how these processes are affected by waveform shape, frequency and the degree of stress biaxiality. To this end, both load (or torque) and strain control tests were performed. The results are found to have important implications not only with respect to understanding crack development in titanium alloys as a whole but also in relation to the development of numerical models to describe these events.

EXPERIMENTAL METHODS

Specimens were manufactured from IMI834 supplied in the form of 30mm round bar. Prior to machining, blanks were heat treated to give a bi-modal microstructure with a retained primary alpha content of 15%. This was achieved by heating in the alpha+beta field (1025°C) for two hours followed by oil quenching, a two hour age at 700°C and air cooling.

Two specimen designs were employed for testing at 20°C. All torsion and combined tension/torsion tests used a tubular specimen while a solid specimen geometry was adopted for uni-axial tension tests (Evans and Bache, 1994). Closed-loop servohydraulic tension-torsion machines provided maximum loading capacities of 50KN axial load and 400Nm torque. Load and torque controlled tests were carried out either under tension, torsion or in phase mixed mode (σ_{11}=σ_{21}) conditions. Sinusoidal loading waveforms of 1Hz and 10Hz frequency were applied. In addition, the designated "cyclic" and "dwell" waveforms, represented schematically in Fig. 1, were assessed, each incorporating a 2 second rise and fall between peak and minimum stress. The one second hold at peak load under cyclic loading was to facilitate data acquisition. Data from the dwell tests were taken shortly before the end of the dwell period. For all loading configurations the R ratio was 0.1 . Extensometry was designed to monitor axial extension and rotational twist from the specimen gauge section when under torsion loading (Bache and Evans, 1992). Tension tests were monitored by means of a commercial strain gauge bridge

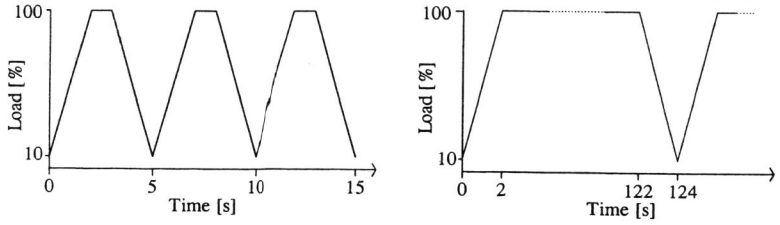

Fig. 1. Cyclic (left) and dwell loading waveforms.

extensometer. Through the application of in-house software, strain-time records and cyclic life were recorded.

The bi-axial extensometer was also used for strain control testing under tension and torsion modes. For tension, two strain ratios, R=0 (zero to maximum) and R=-1 (fully reversed) were evaluated. A triangular waveform with a constant strain rate of 0.5% per second was generated via in-house software which also continually monitored output load and extension throughout individual strain reversals. This provided a record of peak and minimum stress as a function of cycles together with examples of stress-strain hysteresis loops. Failure was defined as a 10% reduction in peak stress below the "stabilised" condition. Where a clear stabilised stress was not attained, (i.e. peak tensile load either continuously increased or decreased throughout the test), the value at half the total life was used for that particular strain range. Similar tests under torsional strain control were at a constant cyclic frequency of 1Hz and R=0.

STRESS AND STRAIN CRITERIA

Modified versions of the von Mises stress and strain criteria have been employed previously by the authors to correlate multi-axial fatigue data. The equations are defined below:

Tension test: $\sigma_{eff} = \sigma_{11} = \frac{P}{A}$ and $\varepsilon_{eff} = \varepsilon_{11} = Ln\frac{(l+e)}{l}$

Torsion test: $\sigma_{eff} = \sqrt{3}\sigma_{21} = \sqrt{3}\frac{3T}{2\pi(r_o^3 - r_i^3)}$ and $\varepsilon_{eff} = \frac{1}{\sqrt{3}}\varepsilon_{21} = \frac{1}{\sqrt{3}}\frac{(r_o + r_i)}{2}\frac{\Theta}{l}$

Combined tension and torsion: $\sigma_{eff} = \sqrt{(\sigma_{11})^2 + 3(\sigma_{21})^2}$

where σ_{eff}=effective stress, ε_{eff}=effective strain, σ_{11} /ε_{11} and σ_{21} /ε_{21} the tensile and shear stress/strain components respectively, P=load, A=cross sectional area, T=torque, r_o and r_i the outer and inner gauge radii and l=gauge length. For the construction of fatigue life curves, failure under tension was taken as complete specimen separation but under torsion a theta creep analysis of strain-time records defined a "life to the onset of tertiary deformation" (Bache and Evans, 1992).

RESULTS

The effect of stress bi-axiality on IMI834 is demonstrated in Fig. 2. The data are from tests conducted with the "cyclic" waveform. On an effective stress basis, this alloy displays a clear dependence on loading mode. Tension loads are more damaging than torsion. The combined tension/torsion mixed mode gives fatigue lives that lie between these two extremes.

The response of the alloy to the different loading waveforms is illustrated for tension in Fig. 3. Sinusoidal tests at both 1 and 10 Hz frequency appear to display comparable fatigue lives and a single best line fit can be drawn through the data. Lives under the "cyclic" waveform fall significantly short of sinusoidal data for the applied stresses in the range 725 to 900MPa. At the low stress end (approaching 700MPa) lives are similar for the different waveforms. For stresses above 900MPa, the combination of data from sinusoidal and cyclic tests indicates a significant break in their respective fatigue behaviour. A best fit line has been constructed for the high stress sinusoidal/cyclic data such that it extrapolates to the measured monotonic

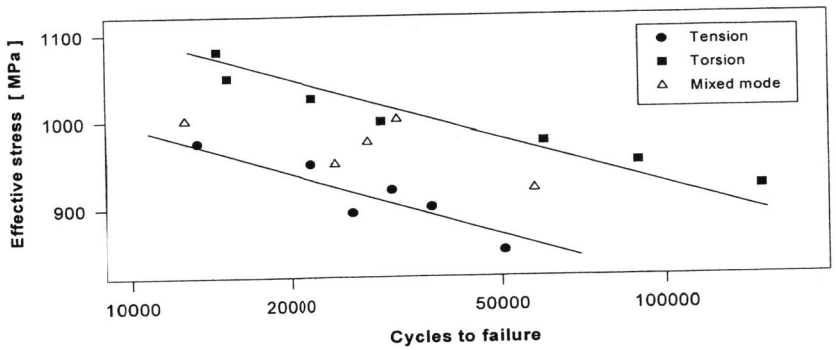

Fig. 2. The effect of stress bi-axiality on IMI834

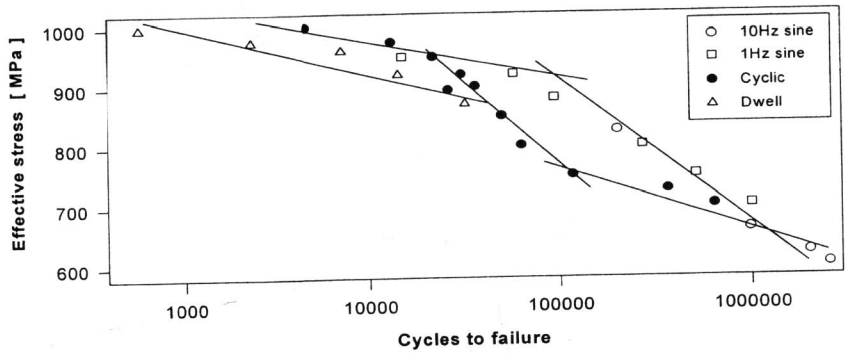

Fig. 3. The effect of waveform on IMI834 under tension.

ultimate strength under tension (1200MPa) at one-half cycle. A similar technique has been employed to draw a line through the 2 minute dwell test data. On this basis, the dwell line intersects the cyclic trend at approximately 875MPa.

The strain control fatigue data for tension and torsion loading are presented in Fig. 4. As in the case of load/torque control, there is clearly a different response for the two modes with fatigue lives significantly lower under uniaxial tension compared with torsion.

Monotonic true stress-true strain curves (MSSC) as measured under tension and torsion are presented in Fig. 5. Employing the modified von Mises criteria clearly gives a good correlation between the two loading modes. Cyclic stress-strain curves (CSSC) derived from strain control fatigue tests are also included in Fig. 5. The torsion data demonstrate a greater degree of work softening compared to tension. Superimposed on the tension curve are two points derived from load control tests conducted under a "cyclic" waveform at stresses of 900 and 920MPa. Records of strain versus cycles for these tests are illustrated in Fig. 6. Taking the strain accumulated at half the total life to represent the "stabilised" condition clearly provides a good correlation between strain and load control cyclic data.

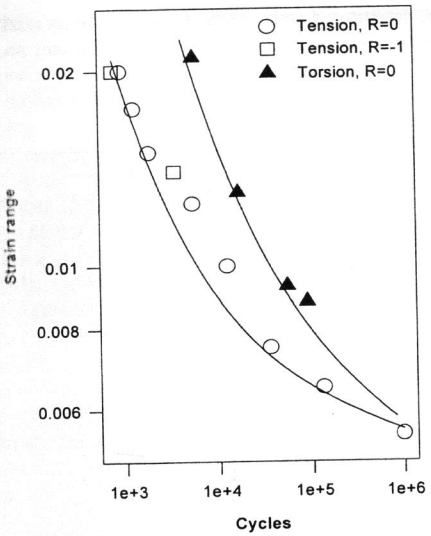

Fig. 4. Strain control fatigue data under tension and torsion.

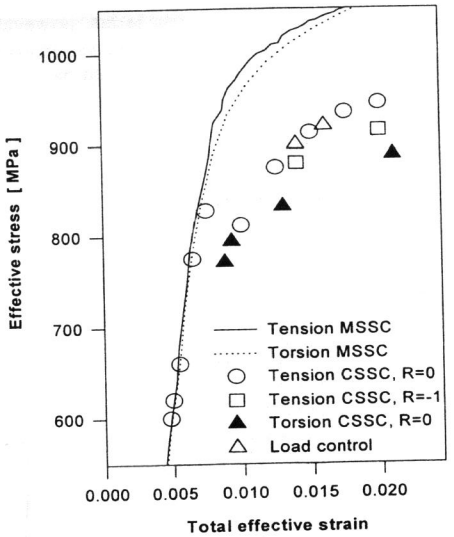

Fig. 5. Monotonic and cyclic stress strain curves under tension and torsion.

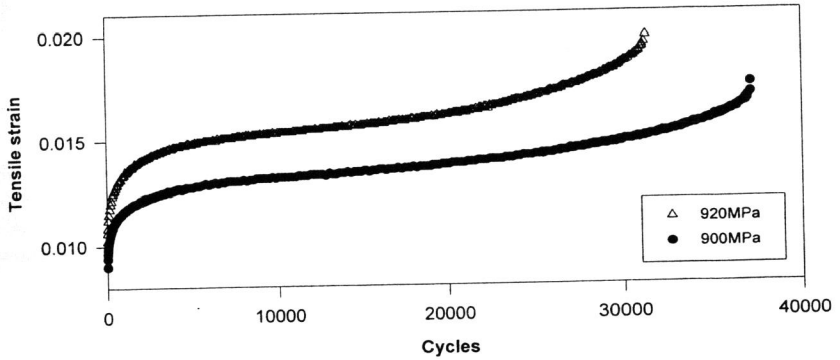

Fig. 6. Strain accumulation under load controlled tension at 900 and 920MPa.

Failures in IMI834 can be divided into two categories according to the magnitude of applied stress. At high stresses/strains features consistent with shear deformation are dominant. Under tensile load slip deformation was evident on the specimen gauge surface and subsurface quasi-cleavage facets were often inclined. Under torsion, flat shear failures occurred which were largely featureless due to abrasion on the fracture plane. At low stress levels, less than monotonic yield, both tension and torsion fractures suggest an increased influence of tensile stress. Tension failures were characterised by facets, on this occasion orientated virtually perpendicular to the tensile stress axis. A characteristic of all facets was the good definition of features on their surface suggesting that there had been little contact during the fatigue life. The facets were typically 20 to 30μm across and therefore comparable in size to the alloy

microstructural unit size. The facets, however, constituted only a small part of the overall fatigue crack area. The main feature was striation dominated Stage II crack growth. The torsion failures change to a helical form with the cracks propagating perpendicular to the maximum principal stress, a fracture path typical of conventional Stage II crack growth. The two extreme forms of torsion failure (flat shear and helical fractures) are illustrated in Fig. 7.

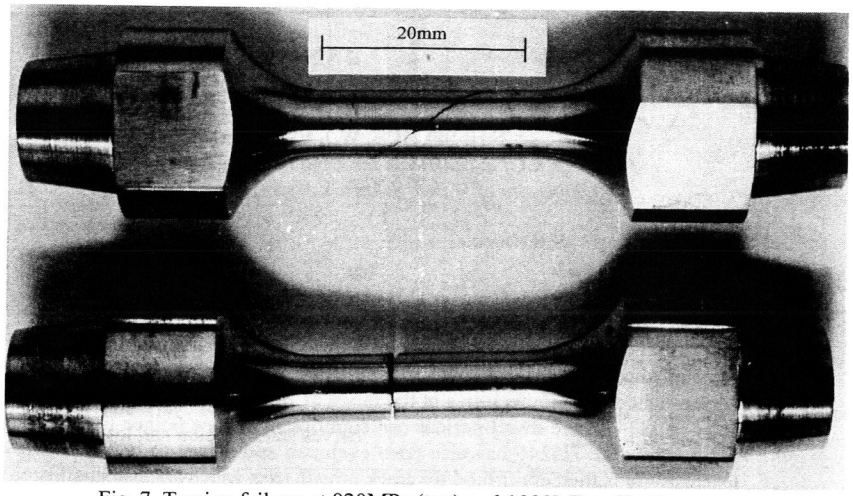

Fig. 7. Torsion failures at 920MPa (top) and 1090MPa effective stress.

DISCUSSION

The observation that cyclic lives under torsion are greater than those in tension for the same effective strain amplitude has been reported previously for other alloy systems (Socie, 1993). Fatemi and Socie (1988) address this difference by introducing a damage model which relates fracture behaviour to a combined expression based on cyclic shear strain and the maximum tensile stress on the plane of maximum shear. The model has the general form:

$$\gamma\left(\frac{1+k\sigma_{n,\max}}{\sigma_y}\right)=\frac{\tau_f}{G(2N)^b}+\gamma_f(2N)^c$$

where γ_f =shear fatigue ductility coefficient, τ_f =shear fatigue strength coefficient, c=fatigue ductility exponent, b=fatigue strength exponent, 2N=the number of reversals to first crack, γ=maximum shear strain amplitude, $\sigma_{n,max}$ =maximum tensile stress perpendicular to plane of shear, σ_y =yield strength, k=constant ~ 1 and G=shear modulus.

On the basis of the information in Fig. 4 and the assumption that the appropriate shear planes are on average at 45° to the tensile axis, the tension and torsion strain control data were replotted according to this critical plane approach. The resultant graph of $\gamma(1 + k\sigma_{n,max}/\sigma_y)$ against cycles is presented in Fig. 8. It is evident that there is now good correlation between the two loading modes.

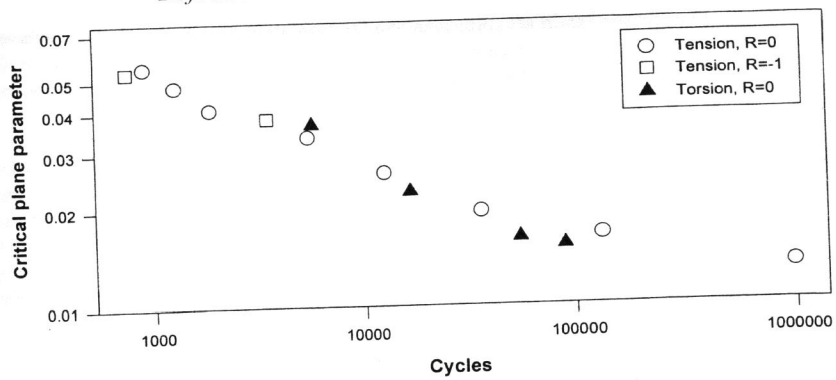

Fig. 8. Strain control fatigue data plotted in terms of a critical plane parameter.

Fatemi and Socie (1988) argue that the model works because of crack closure which could be significant under pure torsion but would be markedly reduced by the action of a tensile stress. It is not clear how relevant the closure argument is to the present situation, but it is well appreciated that the basal plane facets at the early stages of crack growth develop in intense slip bands under the action of a tensile stress (Wocjik et al, 1988). From work on a range of titanium alloys (Bache and Evans, 1992; Evans and Bache, 1994; Bache et al 1995a) it appears that the tensile and shear strain components act together to generate a sufficient level of damage for separation of the slip band. Thus facet formation can occur with a high tensile component and a small amount of slip deformation, average amounts of each or high shear and a small tensile stress. Further, cyclic variations in stress are not essential as facetting can be found after static loading and stress relaxation (Evans, 1987a). In fact, the available data suggest that the necessary condition for facet formation is the accumulation of plastic strain. This view is reinforced by the frequency dependence evident in Fig. 3. The rate of strain accumulation will be greater at the lower frequencies particularly if this is also associated with an unbalanced cycle with a period of dwell at the maximum tensile stress only.

The growth in plastic strain with time is believed to act in a number of ways. Thus, it will lead to intensification of slip bands and thereby promote their eventual separation. More importantly, though, it will be associated with a major redistribution of stress within the alloy. This is particularly relevant to alpha/beta titanium alloys which, due to the restricted number of slip systems available at ambient temperatures, have a highly anisotropic crystallographic structure and consist of an inhomogeneous microstructure due to the two phase heat treatment. In addition, local microstructural variations can result from the processing operations (e.g. basketweave/aligned alpha morphologies). It has been argued previously (Evans, 1987a) that the redistribution process involves a transfer of stress from weak to strong regions within the microstructure. In fact, it has been suggested that the plastic strain accumulation (i.e. low temperature creep) is a consequence of the redistribution process (Evans, 1987b). Figure 6 illustrates how the strain accumulation varies with stress at ambient temperature in the present alloy. Taking the strain at half life in these tests and plotting against applied maximum cyclic stress, the cyclic stress-strain data in Fig. 5 are obtained. This graph also contains cyclic stress-strain curves obtained in the conventional way from hysteresis loops generated under tension and torsion strain control experiments. The close correlation of the tensile stress and tensile strain based data is striking. Essentially, they provide two views of the same event which is

stress redistribution, plastic strain accumulation and the formation of the quasi-cleavage facets from which the fatigue cracks propagate. It is noticeable, that the torsion cyclic stress-strain curve is lower implying that a greater amount of stress redistribution is required for a loading mode in which the ratio of tensile/shear stress component is relatively low.

The fact that the degree of biaxiality affects fatigue response has important implications for crack development at stress concentration features. In previous work on the same alloy, it has been found that a critical strain technique using the Neuber stress redistribution method gives a predicted notch response that falls short of measured data when the tension curve in Figs. 4 and 5 are used, but a prediction that is greater than the measurements for the corresponding torsion curve (Bache et al, 1995b). On the basis of the current work, the critical plane parameter technique and its application to notches is being explored.

CONCLUSIONS

1. The ambient temperature fatigue response of IMI 834 is dependent on stress biaxiality with torsion stress or strain control giving longer lives than the equivalent tension control.
2. A critical plane approach incorporating the maximum shear strain and the tensile stress normal to the plane of shear provides good correlation of tension and torsion response.
3. The critical plane approach is consistent with the known mechanisms of quasi-cleavage facet formation.
4. Facets are a consequence of stress redistribution within the alloy and are associated with plastic strain accumulation.
5. The plastic strain accumulation is responsible for the frequency dependent fatigue response observed.

REFERENCES

Bache, M.R. and W.J. Evans (1992). Tension and torsion fatigue testing of a near alpha titanium alloy. *Int. J. Fatigue,* **14**, 331-337.

Bache, M.R., H.M. Davies and W.J. Evans (1995a). A model for fatigue crack initiation in titanium alloys", *Proc. 8th World Conf. on Titanium,* B'ham, U.K., Institute of Materials.

Bache, M.R., W.J. Evans and G.S. Rees (1995b).Variations in biaxial cyclic stress-strain response of high performance materials. *Proc. of ISABE*, Melbourne, Australia.

Evans, W.J. (1987a). Stress relaxation and notch fatigue in Ti-6Al-4V, *Scripta Met.,* **21**, 1223-1227.

Evans, W.J. (1987b). The influence of microstructure on dwell sensitive fatigue in a near alpha titanium alloy, *Scripta Met.,* **21**, 469-474.

Evans, W.J. and M.R. Bache (1994). Dwell sensitive fatigue under biaxial loads in the near-alpha titanium alloy IMI685, *Int. J. Fatigue*, **16**(7), 443-452.

Fatemi, A and D.F. Socie (1988). A critical plane approach to multiaxial fatigue damage including out of phase loading, *Fat. Fract. Eng. Mat. Struct.*, **11**,149-165.

Socie, D.F., (1993). In: *Advances in Multiaxial Fatigue*, (eds. D.L. McDowell/R. Ellis), ASTM STP1151, 7-36.

Wojcik, C.C., K.S. Chan and D.A. Koss (1988). Stage I fatigue crack propagation in a titanium alloy, *Acta Met.*, **36**,1261-1270.